Colloid Polym Sci (1995) 273:66–75

ORIGINAL CONTRIBUTION

Y. Miyamoto
K. Fukao
H. Miyaji

Small-angle x-ray scattering of isotactic polystyrene

Received: 2 February 1994
Accepted: 30 April 1994

Dr. Y. Miyamoto (✉) · K. Fukao
H. Miyaji
Department of Fundamental Sciences
Faculty of Integrated Human Studies
Kyoto University
Kyoto 606-01, Japan

Abstract Isothermal crystallization process of isotactic polystyrene at 167 °C has been studied by small-angle x-ray scattering. The observed SAXS intensities consist of the two-phase lamellar structure component, the density fluctuation, and the foreign particle components. The profile of lamellar structure component remains unchanged during crystallization while its intensity increases with crystallization. The lamellar structure of isotactic polystyrene is investigated on the basis of the interface distribution function. An interface distribution function is obtained from the lamellar structure component after correcting the effect of the finite thickness of boundary regions between crystalline and amorphous phases. In order to obtain the structure parameters, the "Gaussian correlation model" is used, in which the correlation between the distributions of neighboring crystal and amorphous thicknesses is taken into account. Agreement is satisfactory between the experimental results and the calculations. The structure parameters of isotactic polystyrene are determined for isothermal crystallization at 167 °C as follows: the average and the standard deviation of crystal thickness are 40 A and 10 A, respectively, those of amorphous thickness are 70 A and 23 A, and the standard deviation of long period is 31 A.

Key words Isotactic polystyrene
small-angle x-ray scattering
isothermal crystallization – interface distribution function – crystal thickness

Introduction

In polymer crystallization, morphology and growth rate are the two main subjects. We have been studying the variation of long period [1], growth rate [2, 3], and morphology [2, 4] of isotactic polystyrene (itPS) with crystallization temperature, solution concentration, and molecular weight. Crystalline lamellar thickness is an important quantity characterizing polymer crystal morphology. Quantitative values of crystal thickness and its variation with crystallization temperature are required not only in determination of the equilibrium melting temperature by a thermodynamic relation, but also in analyzing the kinetic quantities such as the relation between growth rate and crystal thickness.

Among several methods for measuring crystal thicknesses, small-angle x-ray scattering (SAXS) gives a well-defined number-average of crystal thickness. The main purpose of the present paper is to propose a method to obtain information on the two-phase lamellar structure (crystalline and amorphous) from SAXS intensity, i.e., the

distributions of crystal thickness, amorphous thickness, and long period. In SAXS studies of semi-crystalline polymers, it is well known that the lamellar structure component and the density fluctuation component contribute to the observed intensity [5, 6]. In many polymers, besides the density fluctuation component, the specimen in the amorphous state or in the melt gives an additional intensity decreasing with increasing scattering angle, which is attributed to be due to foreign particles [7]. In order to clarify the lamellar structure component, SAXS intensity has been measured during isothermal crystallization process.

There are two approaches in determining the structure parameters from SAXS intensity: a) the direct method in which the comparisons between experimental results and calculations are made directly from a structure model [8] and b) the Fourier transform method in which the comparisons are made in a Fourier-transformed space; in this method are included the correlation function [9, 10, 11] and the interface distribution function [6]. In the direct method, a priori assumptions are necessary for the distributions of amorphous and crystal thicknesses and their correlations in constructing a structure model. Almost all the analyses by the direct method so far have been based on the paracrystal theory, in which the distribution of crystal thickness is assumed to be independent of that of amorphous thickness. The Fourier transform method, on the other hand, needs less assumptions, but correlation functions or, in particular, interface distribution functions can be only approximately obtained because of the limited range of scattering angles available for a Fourier transform. In this work, therefore, the approximate values of structure parameters are determined by a Fourier transform method and refined by the direct method.

The correlation function method proposed by Strobl and Schneider [10] is a powerful tool for the lamellar structure analysis, in which structure parameters are determined by the geometrical interpretations of correlation functions. However, when the average value of the smaller of crystal and amorphous thicknesses is small and its distribution is not narrow enough, correlation functions do not clearly show the "self-correlation triangle"; neither the "central linear section" nor the "base line" is clear in the present case. The interface distribution function is known to be useful for determining the distributions of crystal and amorphous thicknesses, but its applications are still few (recent studies: refs. [12, 13]). Difficulties in the analyses based on the interface distribution function lie in, firstly, that accurate intensity is necessary at high scattering angles between SAXS and wide-angle x-ray diffraction, at which x-ray scattering intensity is smallest, and, secondly, that positive and negative contributions to an interface distribution function usually overlap, so that the decomposition of this function into each component is not straightforward. Accordingly, we have measured x-ray intensity up to high scattering angles and the interface distribution function obtained has been decomposed by a structure model in which a Gaussian correlation is assumed between the distributions of neighboring crystal and amorphous thicknesses.

We first show the experimental results during isothermal crystallization of itPS and discuss the separation of the lamellar structure component from the observed intensity. The resulting intensity is analyzed on the basis of the interface distribution function. The "Gaussian correlation model" is used to determine the structure parameters and the results are examined by comparing the experimental intensity with calculations.

Experimental

The material used was itPS ($Mw = 1.57 \times 10^6$, $Mw/Mn = 6.4$ and 97.2% isotactic triad) purchased from Polymer Laboratories Ltd.

SAXS measurements were carried out at the High Intensity X-Ray Laboratory of Kyoto University. The x-ray is Ni-filtered CuK_α from a fine-focus x-ray generator (RU1000C3, Rigaku Corporation, Japan) operated at 40 kV × 50 mA. Scattered intensities were recorded with a Franks-type point-focusing camera using a two-dimensional position-sensitive proportional counter. The detailed specifications of the equipment have been given elsewhere [14]. The measurements were made at two sample-to-detector distances, 1640 and 640 mm, to cover the range of scattering angle from 0.003 to 0.136 rad. The peak positions of 110 Bragg reflection and amorphous halo are expected to be observed at about 0.14 and 0.15 rad. at 167 °C, respectively. After subtraction of the background intensity and correction for the non-uniformity of detector sensitivity, the isotropic two-dimensional intensity was circularly averaged to give the one-dimensional intensity. The one-dimensional intensities obtained at different camera distances were corrected for absorption, the camera distance, the incident beam intensity and the sample thickness, to give the observed intensity $I_{obs}(s)$, where $s = 2\sin\theta/\lambda$ is the magnitude of scattering vector, with the scattering angle 2θ and the x-ray wavelength λ.

In the measurements during the crystallization process, the sample of 1.1 mm in thickness was placed in an evacuated heating chamber, melted at 260 °C for 5 min, and then cooled at a rate of about 30 K/min to a crystallization temperature T_x of 167 °C, at which the fluctuation of temperature is ± 0.2 °C and the accuracy of absolute value, $^{+6}_{-2}$ °C. A crystallization temperature of 167 °C was chosen because the overall crystallization rate of itPS is

the fastest at about 170 °C and the typical spherulite morphology is observed by optical microscopy. The exposure time is 600 s. The crystallization time given below is the center time of exposure. Since the measurements were carried out twice at different camera distances, the overall crystallization rate must be strictly controlled; careful attention has been paid to the sample history up to reaching the crystallization temperature.

Results and discussion

The intensity due to lamellar structure

Figure 1 shows the change in observed intensity $I_{obs}(s)$ with crystallization time t_x, in a log-log scale. No change in SAXS intensity was observed for 30 min after quenching to the crystallization temperature. Optical microscopy showed, however, the growth of spherulites immediately after quenching to the crystallization temperature. Optical microscopy showed, however, the growth of spherulites immediately after quenching from the melt [3]. The diameters of spherulites are 16 μm at $t_x = 30$ min. at 167 °C, but the number of nuclei was so small that the amount of lamellar structure was not sufficient to be detected by SAXS measurements. It is clearly seen from Fig. 1 that the lamellar structure component $I(s)$, of which the peak is situated at $\log s(A^{-1}) \simeq -2.1$, increases and the density fluctuation component $I_f(s)$ observed at large s-values decreases as crystallization proceeds. In the supercooled liquid state ($t_x = 18$ min. in Fig. 1), besides the density fluctuation component $I_f(s)$, strong intensity $I_x(s)$ is observed at low scattering angles, which is supposed to be due to foreign particles [7].

In order to separate $I(s)$ from $I_{obs}(s)$, the components $I(s)$, $I_f(s)$ and $I_x(s)$ are assumed to be additive:

$$I_{obs}(s) = I(s) + I_f(s) + I_x(s) , \quad (1)$$

and the component $I_x(s)$, to be independent of the fraction of lamellar structure. We have determined the density fluctuation component $I_f(s)$ by the method proposed by Ruland et al. [15, 16]:

$$I_f(s) = A_f \cdot \exp(B_f s^2) , \quad (2)$$

where A_f and B_f are constants but depend on the fraction of lamellar structure χ. Since $I_{obs}(s)$ in the amorphous state $I_{obs}(s; \chi = 0)$ decreases with the power of s with an exponent of about -2 at small s-values (Figure 1), $I_{obs}(s; \chi = 0)$ is assumed to be expressed by

$$I_{obs}(s; \chi = 0) = I_f(s; \chi = 0) + C_a s^{-D_a} , \quad (3)$$

where C_a and D_a are constants and $I_f(s; \chi = 0)$ is the intensity $I_f(s)$ at $\chi = 0$. The constants A_f, B_f, C_a and D_a are determined by the least square method in the s-range from 0.005 to 0.075 A^{-1} (Fig. 2; $D_a = 2.01$). Then the foreign particle component $I_x(s)$ was determined by

$$I_x(s) = I_{obs}(s; \chi = 0) - I_f(s; \chi = 0) \quad (4)$$

for s-values smaller than 0.06 A^{-1} and extrapolated to large s-values by $C_a s^{-D_a}$.

For the intensities during crystallization process at $t_x > 30$ min., A_f and B_f are determined from the linear relation at large s-values from 0.05 to 0.07 A^{-1} between $\log(I_{obs}(s) - I_x(s))$ and s^2 (Fig. 3 for $t_x = 20$ h). Figure 4 shows the contributions of $I_f(s)$ and $I_x(s)$ to $I_{obs}(s)$ for $t_x = 20$ h. The intensity due to lamellar structure $I(s)$ cor-

Fig. 1 Crystallization time dependence of SAXS intensity at 167 °C. ●: $t_x = 18$ min., ▽: 60, ◇: 120, □: 180, △: 300 and ○: 1200 min. Ordinate is in arbitrary unit

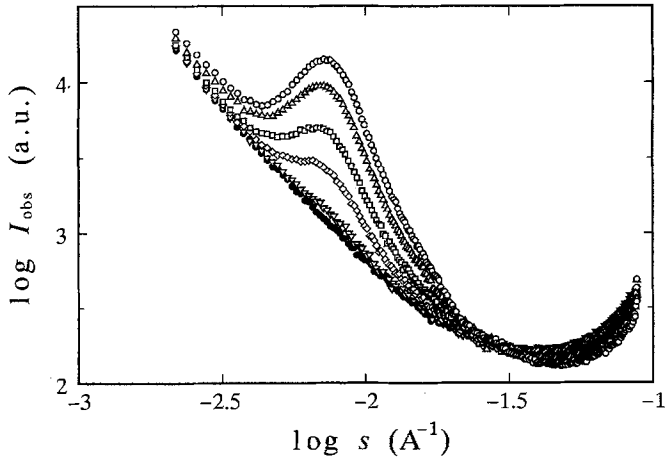

Fig. 2 Determination of the foreign particle component $I_x(s)$ from the intensity in the amorphous state. ○: $I_{obs}(s)$ at $t_x = 18$ min., solid line: calculation by Eq. (3), broken line: $I_f(s)$ in the amorphous state, □: $I_x(s)$ and single dotted line: extrapolation to larger s-values

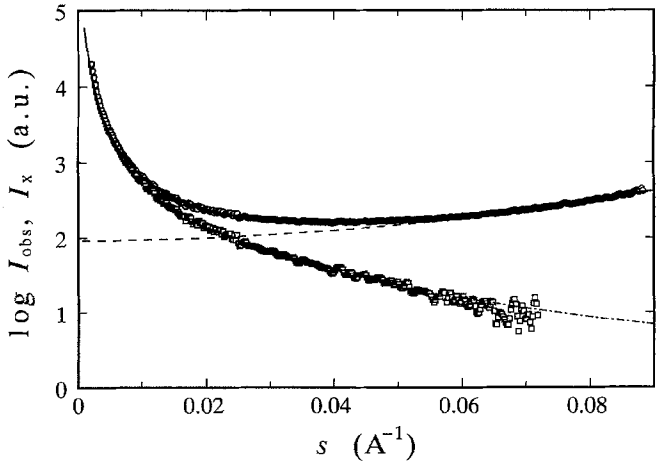

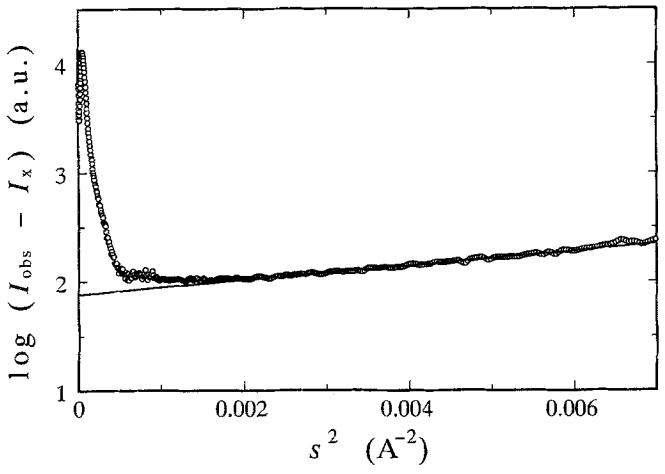

Fig. 3 Determination of the density fluctuation component $I_f(s)$ at $t_x = 20$ h. Solid line shows $I_f(s)$ at 20 h

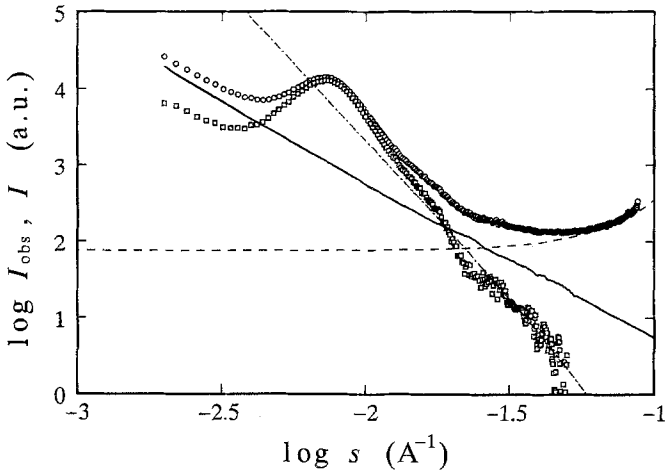

Fig. 4 SAXS intensity at $t_x = 20$ h at 167 °C. ○: $I_{obs}(s)$, □: $I(s)$, solid line: $I_x(s)$, broken line: $I_f(s)$ and single dotted line: $K_p\exp[-2(2\pi sd)^2]/(2\pi)^3 s^4$ (see Eq. (12))

rected for the Lorentz factor s^2 is shown in Fig. 5 normalized by the peak value at each crystallization time for $t_x \geq 120$ min.; the profile of the intensity hardly depends on crystallization time. This indicates that the scattering volume of the lamellar structure increases with crystallization without changing the structure at $T_x = 167$ °C and suggests that the assumptions made in decomposing the observed intensity are reasonable.

Figure 6 shows the dependence of the integrated intensity Q' from $|s| = 0.005$ to 0.03 and A_f on crystallization time; the coefficient B_f showed a change similar to A_f. The coefficient A_f is proportional to the sample density and the compressibility, and B_f is proportional to the intensity of amorphous halo at the low-angle part. Closer examination of Fig. 5 shows that the peak position in $s^2I(s)$ slightly shifts to higher scattering angles with t_x. This small change

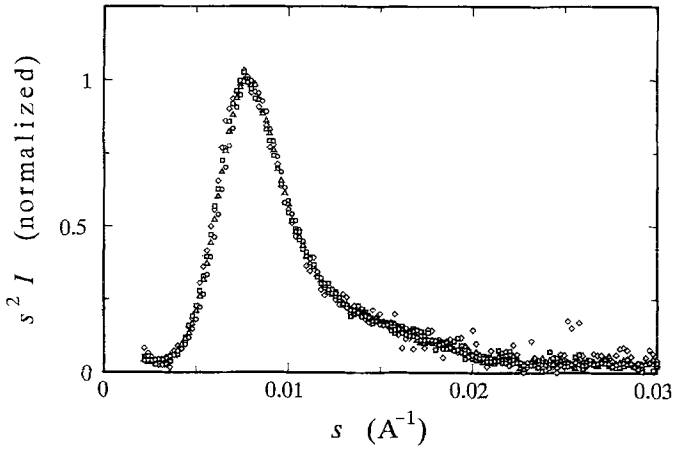

Fig. 5 Lorentz-factor corrected intensity $s^2I(s)$ normalized by the peak intensity. The symbols are the same as Fig. 1

Fig. 6 Dependence of the integrated intensity Q' and the coefficient A_f on t_x at 167 °C

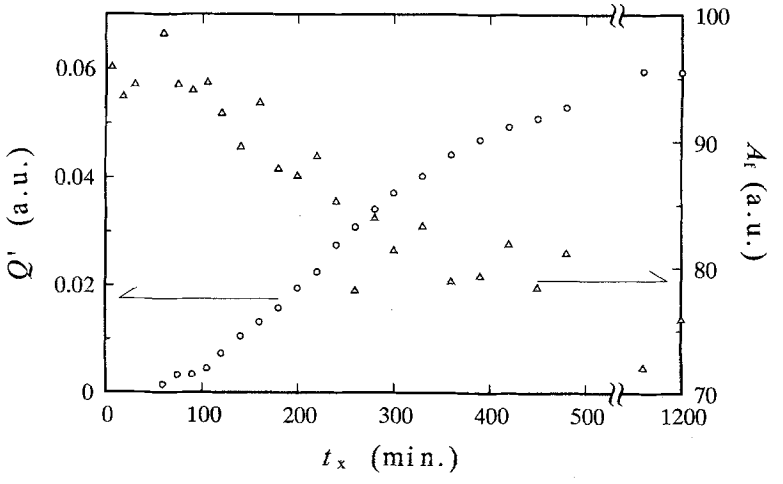

in profile with t_x is supposed to be the effects of the secondary crystallization. In the following discussion the structure parameters will be determined from $I(s)$ at $t_x = 20$ h, at which the lamellar structure component has the least statistical errors.

Linear model and interface distribution function

The sample under investigation is unoriented and represented by an ensemble of isotropically distributed stacks of lamellae. The linear model assumes that the change in electron density in a single stack is expressed by an electron density function $\rho(z)$ which depends only on z, where z is a coordinate in the direction normal to the phase boundary surface in a stack; the lamellar surfaces are parallel and the dimensions of the stacks parallel to the lamellar surfaces are large. We further assume that the number of lamellae in a stack is large enough to be effectively infinite, though the effects of the finite stack are easily taken into account [17].

The effects of deviations from the linear model on SAXS intensity have been discussed: bending and nonparallelism of lamellae and corrugations of boundary surfaces [6, 10, 18]. It has been shown that the effects of deviations are negligible so are as the distances over which lamellae can be regarded as planar are large compared to distances in question such as interlamellar distances. In regard to the effect of the finite stack size in z direction, the analyses taking account of the finite number of crystalline lamellae N in a stack often gave an unreasonable low value for N of 1 or 2. In the case of itPS, Warner et al. gave the results for N of about 2 [19]; they regarded N as a disorder parameter rather than a physical reality. Electron microscopy by Bassett and Vaughan [20, 21] demonstrated that the lamellar structure develops from the very early stage of crystallization and a large number of crystalline lamellae stack each other. Since the effect of finite N becomes negligible if N is 10 or larger [22], we neglect the finiteness in N in the following treatments.

The interface distribution function has been introduced and discussed by Ruland [6]. In this section, we briefly review the analysis based on the interface distribution function in accordance with our present treatments. The change in electron density $\rho(z)$ in an atomic scale is neglected and the electron density well inside the crystalline and amorphous phases are expressed by ρ_c and ρ_a, respectively. In the linear model, the electron density $\rho(z)$ in a single stack is expressed by

$$\rho(z) = \rho_a + \Delta\rho \sum_{j=1}^{\infty} \delta(z - z_j) * b_j(z) , \tag{5}$$

where $\Delta\rho = \rho_c - \rho_a$, z_j is the position of j-th interface, $b_j(z)$ expresses the change in electron density at j-th interface, $\delta(z)$ is the Dirac delta function and $*$ denotes a convolution. If the interface at z_{2j} is the one from amorphous to crystal phase in the positive z direction, $b_{2j}(z)$ is $\pm 1/2$ as $z \to \pm\infty$ and the distance over which $b_{2j}(z)$ changes from $-1/2$ to $+1/2$ is expected to be small compared to crystal and amorphous thicknesses. We assume for simplicity that $b_j(z)$ is an odd function, of which the origin defines the position of z_j. If the distribution of $b_j(z)$ is independent of that of z_j, the lamellar structure component $I(s)$ is given, except near origin, by

$$2\pi s^2 I(s) = K_p[(\langle|f_b|^2\rangle - |\langle f_b\rangle|^2) + |\langle f_b\rangle|^2 Z(s)] , \tag{6}$$

where K_p is a constant proportional to $(\Delta\rho)^2$ and the specific inner surface, and $f_b(s)$ is the structure factor of interface given by the Fourier transform of $b_j(z)$. The lattice factor or the interference function for interface $Z(s)$ is given by

$$\begin{aligned} Z(s) &= \sum_{n=-\infty}^{\infty} (-1)^n \langle \exp(2\pi i s \Delta z_n)\rangle \\ &= \sum (-1)^n \mathscr{F}[h_n(z)] \\ &= \sum (-1)^n H_n(s) , \end{aligned} \tag{7}$$

where Δz_n is the distance between interfaces of n-separation, $z_{j+n} - z_j$, and its distribution is assumed to be independent of j, $h_n(z)$ is the distribution function of Δz_n and $H_n(s)$ is the Fourier transform ($\mathscr{F}$) of $h_n(z)$. In Eqs. (6) and 7, $\langle X\rangle$ is the statistical average of X, in the present case, the average with respect to the number of interfaces.

The interface distribution function $g(z)$ is defined by

$$g(z) = \sum_{n=-\infty}^{\infty} (-1)^n h_n(z) , \tag{8}$$

and given by the Fourier transformation of $Z(s)$. When the distributions of the electron density change at phase boundary regions are neglected and the equation

$$b_j(z) = (-1)^j \langle b_{2j}(z)\rangle \equiv (-1)^j b(z) \tag{9}$$

holds, as will be assumed in the subsequent section, Eq. (5) reduces to

$$\rho(z) = \rho_a + \Delta\rho \sum_{j=1}^{\infty} (-1)^j \delta(z - z_j) * b(z) \tag{10}$$

(see Fig. 7). Hence, $g(z)$ represents the correlation function of the delta functions at the positions of interface with a positive sign for an amorphous to crystal interface and a negative one for a crystal to amorphous interface. For the convenience of the following discussion, we define $h_n^c(z)$ as the distribution function of the distances separated by n delta functions ($n > 0$) starting from a plus delta function in the positive z direction and $h_n^a(z)$ as that from a minus

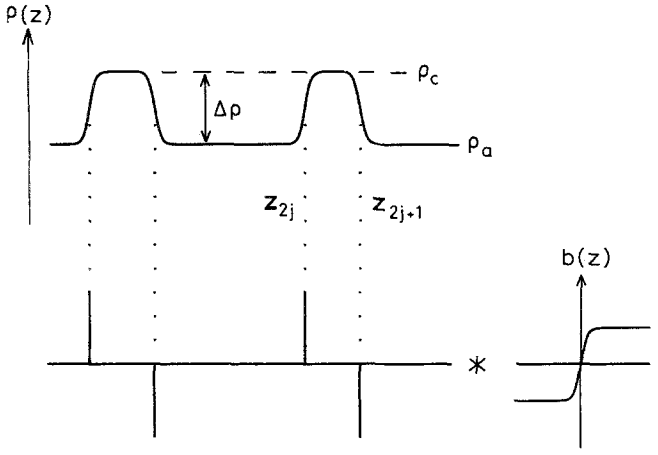

Fig. 7 Schematic representation of one-dimensional electron density

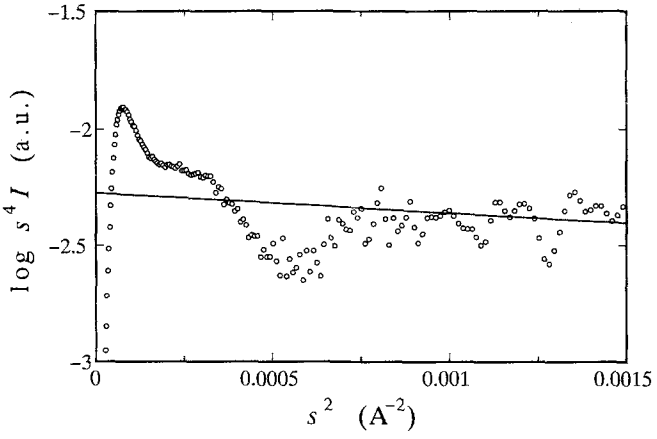

Fig. 8 Determination of the thickness of boundary region (t_x = 20 h)

delta function, and for simplicity $h^{y}_{-n}(z)$ is defined to be equal to $h^{y}_{n}(-z)$ (y = c, a); $h_n(z)$ is given by $(h^{c}_{n}(z) + h^{a}_{n}(z))/2$. The distribution of crystal thickness c, $h_c(c)$, is defined to be equivalent to $h^{c}_{1}(c)$ and that of amorphous thickness a, $h_a(a)$, equivalent to $h^{a}_{1}(a)$; the crystal thickness c refers to the distance between the interfaces, but not to the core thickness.

Determination of interference function $Z(s)$

In order to determine $Z(s)$ from Eq. (6), information on $b_j(z)$ or its Fourier transform is necessary. As mentioned in the preceding section, the distributions in the electron density change at boundary regions are neglected; the first term in the bracket in Eq. (6) is zero. The slope of $\log I(s)$ vs. $\log s$ in Fig. 4 is slightly steeper than -4 at large s-values. This deviation from Porod's law indicates the boundary surfaces are diffuse. We assume that $f_b(s)$ is expressed by

$$f_b(s) = i \cdot \frac{\exp[-(2\pi s d)^2]}{2\pi s}, \tag{11}$$

where d is a parameter representing the thickness of boundary region. When the trapezoidal electron density with a boundary thickness of d_t is assumed for a crystalline layer, i.e., $b(z) = z/d_t$ for $-d_t/2 < z < d_t/2$, d_t is given by $\sqrt{24}d$ [5, 6].

The details of the distributions and the form of functions of $b_j(z)$ should appear in $I(s)$ at high scattering angles of the order of $s \sim 1/d$. The assumptions made on $b_j(z)$ so far imply that $b_j(z)$ is symmetric regarding the position of interface (odd function), the distribution of electron density change at each interface is neglected (Eq. (9)) and the average $b(z)$ is expressed by an error function

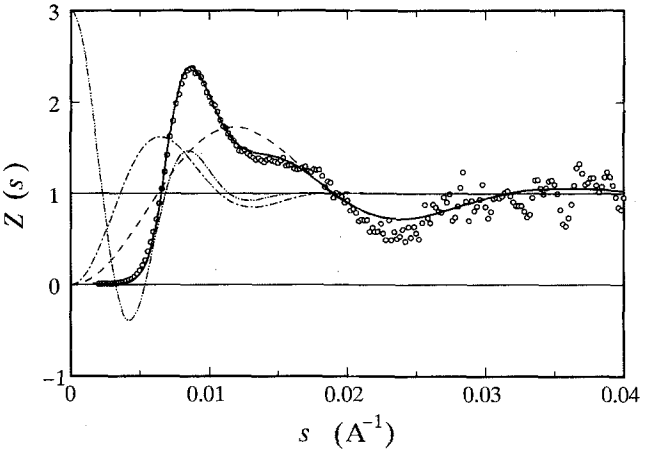

Fig. 9 Interference function $Z(s)$ at t_x = 20 h. ○: experimental, solid line: calculation, broken line: $-(H^{c}_{1} + H^{c}_{-1})/2 + 1$, single dotted line: $-(H^{a}_{1} + H^{a}_{-1})/2 + 1$ and double dotted line: $(H_2 + H_{-2})/2 + 1$

(Fourier transformation of Eq. (11)). These assumptions had to be made because the accurate values of $I(s)$ at $s \sim 1/d$ were not available in the present study due to the corrections for $I_x(s)$ and $I_f(s)$.

From Eqs. (6), (9) and (11), the interference function $Z(s)$ is given by

$$Z(s) = (2\pi)^3 s^4 \cdot I(s) \exp[2(2\pi s d)^2]/K_p . \tag{12}$$

Since $Z(s)$ is expected to approach unity at large s-values, the values of K_p and d are determined from the linear relation in $\log s^4 I(s)$ vs. s^2 plot in the range of s from 0.03 to 0.04 A^{-1}, as shown in Fig. 8; the value of d is 1.6 A, corresponding to $d_t \simeq 8$ A in the linear density change at the boundary. The interference function $Z(s)$ is determined by Eqs. (12) and shown in Fig. 9. The factor

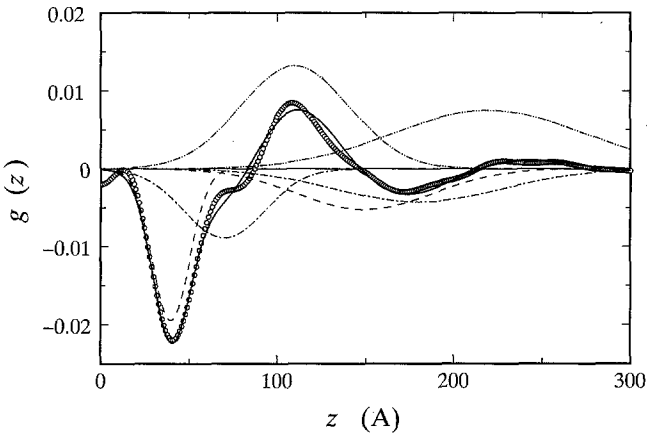

Fig. 10 Interface distribution function at $t_x = 20$ h. ○: experimental, solid line: calculation, broken line: $-h_1^c/2$ (negative peak at ca. 40 A) and $-h_3^c/2$ (at ca. 150 A), single dotted line: $-h_1^a/2$ (negative peak at ca. 70 A) and $-h_3^a/2$ (at ca. 180 A), and double dotted line: h_2 (positive peak at ca. 110 A) and h_4 (at ca. 220 A)

$K_p \exp[-2(2\pi sd)^2]/(2\pi)^3 s^4$ is shown in Fig. 4 by a single dotted line. The interface distribution function $g(z)$ is obtained by the Fourier transformation of $Z(s)$ (Fig. 10). On the calculation, an extrapolation of the experimental data to $s = 0$ was made by a linear connection between the origin and the first measured point in $s^2 I(s)$ vs. s scale and $Z(s) - 1$ was Fourier-transformed, of which the difference by one corresponds to a self-correlation part, $h_0(z)$, the delta function at the origin.

Correlation between neighboring crystal and amorphous thicknesses

Since the crystallinity of itPS is less than 0.5 from the density measurements [23], the negative peak observed in Fig. 10 at about 40 A is considered to represent the distribution of crystal thickness $h_c(z)$ or $h_1^c(z)$ and is approximated by a Gaussian near the minimum. Figure 10 shows that the distance distributions overlap even at small distances, so that the decomposition of $g(z)$ into $h_n^c(z)$ and $h_n^a(z)$ should be dealt with by invoking a structure model. The most appropriate starting model will be the paracrystal model in which the distribution $h_c(z)$ is assumed to be independent of $h_a(z)$.

In this case, $h_n^c(z)$ and $h_n^a(z)$ are given by

$$h_{2j+1}^c(z) = h_c * (h_c *^j h_a)$$
$$h_{2j+1}^a(z) = h_a * (h_c *^j h_a)$$
$$h_{2j}^c(z) = h_{2j}^a(z) = (h_c *^j h_a)\,, \tag{13}$$

where $*^j$ denotes j times convolution. A well-known formula [8] is readily obtained for the interference function $Z(s)$ from Eqs. (7) and (13):

$$Z(s) = \Re\left[\frac{(1 - H_c)(1 - H_a)}{(1 - H_a H_c)}\right], \tag{14}$$

where $\Re[X]$ is the real part of X, and $H_c(s)$ and $H_a(s)$ are the Fourier transforms of $h_c(z)$ and $h_a(z)$, respectively. Agreement was poor between the experimental results and the calculations based on the paracrystal model with Gaussian distributions for $h_c(z)$ and $h_a(z)$ both in a $g(z) - z$ plot by Eqs. (8) and (13), and in a $Z(s) - s$ plot by Eq. (14). In this paracrystal model, four structure parameters were employed; the average thicknesses $\langle c \rangle$ and $\langle a \rangle$, and the standard deviations σ_c and σ_a, for $h_c(z)$ and $h_a(z)$, respectively.

For the improvement of a structure model, deviations from Gaussian distributions and a correlation between distance distributions should be taken into account; a single-modal distribution may well hold for each distance distribution because of the isothermal crystallization condition. Since $h_1^c(z)$ seems to be approximated by a Gaussian (Fig. 10), we have examined the effects of the correlation between neighboring crystal and amorphous thicknesses on $g(z)$ and $I(s)$. Let $g_n(z_1, z_2, \cdots, z_n) \equiv g_n(\{z_j\})$ be the n-successive-distance distribution, where z_j's are alternating crystal and amorphous thicknesses, $\cdots, a_{j-1}, c_j, a_{j+1}, c_{j+2}, \cdots$; note the definition of z_j has changed from Eq. (5). Because $h_n(z)$ is the distribution function of $z = \sum_{j=1}^{n} z_j$, $H_n(s)$ is expressed by

$$H_n(s) = \int \cdots \int g_n(\{z_j\}) \prod_{j=1}^{n} \exp(2\pi i s z_j) dz_j\,. \tag{15}$$

Since we take only the neighboring-thickness correlation into account, $g_n(\{z_j\})$ is approximated by the two-distance distribution $g_2(z_1, z_2)$:

$$g_n(\{z_j\}) = \frac{\prod_{j=1}^{n-1} g_2(z_j, z_{j+1})}{\prod_{j=2}^{n-1} g_1(z_j)}\,, \tag{16}$$

where $g_1(z_j)$ is given by

$$g_1(z_1) = \int g_2(z_1, z_2) dz_2\,. \tag{17}$$

Given $g_2(z_1, z_2)$, therefore, $H_n(z)$ is obtained by Eqs. (15), (16) and (17), and hence $h_n(z)$ and $g(z)$.

Gaussian correlation model

Here, we assume a Gaussian for a two-distance distribution function g_2. Hereafter the arguments in $g_2(c, a)$ are taken as neighboring crystal thickness c and amorphous one a, rather than the order of the thickness sequence.

Namely,

$$g_2(c, a) = A\exp[\{\alpha(c - \langle c\rangle)^2 - 2\gamma(c - \langle c\rangle)(a - \langle a\rangle) + \beta(a - \langle a\rangle)^2\}] , \quad (18)$$

where A is a normalization factor and α, β, and γ are constants; γ represents the correlation between crystal and amorphous thicknesses. The distance distributions $h_c(c)$, $h_a(a)$ and $h_l(l)$ which is the distribution function of long period l, are given by

$$h_c(c) = \int g_2(c, a)da$$

$$h_a(a) = \int g_2(c, a)dc$$

$$h_l(l) = \int g_2(c, a)\delta(l - c - a)dcda , \quad (19)$$

and from Eqs. (15–17) all the distance distributions functions $h_n^y(z)$ are Gaussians (y = c, a). The average value of $h_n^y(z)$, $\langle z_n^y\rangle$ is given by

$$\langle z_{2j+1}^c\rangle = \langle c\rangle + j(\langle c\rangle + \langle a\rangle)$$

$$\langle z_{2j+1}^a\rangle = \langle a\rangle + j(\langle c\rangle + \langle a\rangle)$$

$$\langle z_{2j}^c\rangle = \langle z_{2j}^a\rangle = j(\langle c\rangle + \langle a\rangle) . \quad (20)$$

Because the correlation between $h_c(c)$ and $h_a(a)$ is taken into account, one more structure parameter, the standard deviation of $h_l(l)$, σ_l, has to be introduced than in the case of the paracrystal model. From Eqs. (15) and (16), the standard deviation of $h_n^c(z)$, σ_n^c is given by recurrence relations:

$$(\sigma_{2j+1}^c)^2 = (\sigma_{2j}^c)^2 + (\beta D + 2\gamma D v_{2j})/2$$

$$(\sigma_{2j+2}^c)^2 = (\sigma_{2j+1}^c)^2 + (\alpha D + 2\gamma D v_{2j+1})/2$$

$$v_2 = 1 + \gamma/\alpha$$

$$v_{2j+1} = 1 + v_{2j}\gamma/\beta$$

$$v_{2j+2} = 1 + v_{2j+1}\gamma/\alpha , \quad (21)$$

where D and the constants in Eq. (18) are expressed by

$$D = 2(\sigma_c^2 + \sigma_a^2)\sigma_l^2 - \sigma_l^4 - (\sigma_c^2 - \sigma_a^2)^2$$

$$\alpha = 2\sigma_a^2/D$$

$$\beta = 2\sigma_c^2/D$$

$$\gamma = (\sigma_l^2 - \sigma_c^2 - \sigma_a^2)/D$$

$$A = 1/\pi\sqrt{D} . \quad (22)$$

For σ_n^a, the recurrence relations are obtained by interchanging α and β in Eq. (21).

We will determine the structure parameters $\langle c\rangle$, $\langle a\rangle$, σ_c, σ_a and σ_l by decomposing $g(z)$ into $h_n^y(z)$ (y = c, a) on the basis of the Gaussian correlation model. Because of the corrections for $I_x(s)$ and $I_f(s)$, and the evaluation of $|f_b|^2$, the accuracy of $Z(s)$ becomes poorer with increasing s-value. As a result, the limiting s-value available for a Fourier transformation was about 0.03 A^{-1} and oscillations due to cut off are observed in Fig. 10. We have, accordingly, decomposed $g(z)$ in Fig. 10 into the Gaussians representing $h_n^y(z)$, of which the average and the standard deviation are regarded as approximate values. The result of fitting by the use of Eqs. (8) and (20–22) is shown in Fig. 10 by a solid line; the components $h_n^y(z)$ are also shown by broken and dotted lines for $n \leq 4$.

The values of structure parameters are finally determined by fitting $Z(s)$ with the values obtained above as the initial approximate values. The interference function $Z(s)$ is calculated by Eqs. (7), (15) and (20–22), and the result is shown in Fig. 9 by a solid line. The values of structure parameters are $\langle c\rangle = 40$, $\langle a\rangle = 70$, $\sigma_c = 10$, $\sigma_a = 23$ and $\sigma_l = 31$ (unit is in angstrom). The fitting was made by a trial-and-error method and the parameter values are determined by minimizing the square deviation in the s-range from 0.005 to 0.022 A^{-1}. The components $H_n^y(s)$ are shown in Fig. 9 by broken and dotted lines for $|n| \leq 2$; $H_0(s)$ is constant (unity) and each component shown in Fig. 9 is added by one for facilitating the comparison with the experimental results. It is worth noting that the values of $Z(s)$ near the second maximum or shoulder are dominated by $H_1^c(s)$, or more precisely $(H_1^c(s) + H_{-1}^c(s))/2$ or $\Re[H_1^c(s)]$, rather than the second peak in $H_2(s)$. We roughly explain how the structure parameters are determined from $Z(s)$. Because $H_1^c(s)$ is dominant at large s-values, the oscillation and the dumping of $Z(s)$ at s-value larger than 0.015 A^{-1} give $\langle c\rangle$ and σ_c. The position and the height of the first maximum in $Z(s)$ give $\langle c\rangle + \langle a\rangle$ and a combined value of σ_c, σ_a, and σ_l. The concaveness between the first and second maxima also gives a combined value of σ_c, σ_a and σ_l.

The intensity $s^2I(s)$ is reproduced in Fig. 11 by Eqs. (6), (7) and (11); agreement between the experimental results and the calculations is satisfactory. Disagreement at s-value smaller than 0.005 A^{-1} is a result of the intensity at small scattering angles in Fig. 4. The origin of the intensity at low s-values is not clear at present; this intensity may suggest the effects of deviation from the linear model or the effects of the finite stack size or the small dependence of $I_x(s)$ on χ, or it may be due to other sources which are not considered in this work.

The effects of the asymmetric distance distributions have not taken into account. The experimental and calculated results shown in Figs. 9 and 11 indicate that the effects of asymmetry are small in the present crystallization condition. Since the position of the first maximum and the oscillation at large s-values in $Z(s)$ are clear in Fig. 9, the averages $\langle c\rangle$ and $\langle a\rangle$ are correctly determined. Small discrepancies between the experimental intensity and the calculated one at about $s = 0.015 - 0.02$ A^{-1} in Fig. 9 are

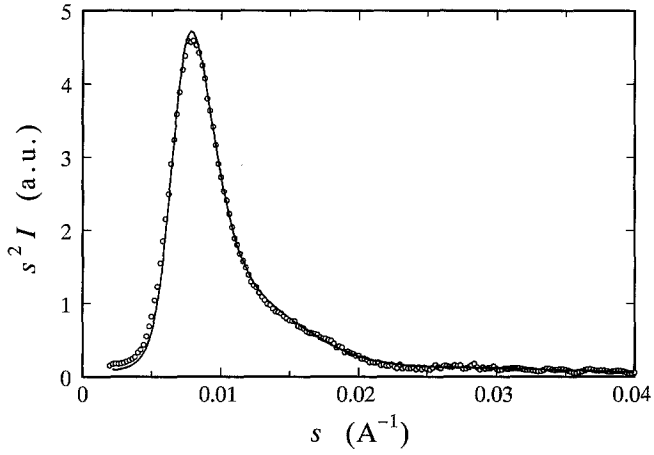

Fig. 11 Lorentz-factor corrected intensity due to lamellar structure at $t_x = 20$ h ○: experimental, solid line: calculation

supposed to be due to the effects of asymmetric distribution in $h_c(z)$. The values of standard deviations give the correlation coefficient of 0.7, which indicates the strong positive correlation between the distributions of neighboring crystal and amorphous thicknesses. However, since the above value of the correlation coefficient is obtained on the basis of the Gaussian correlation model, the further examinations will be necessary on the effects of asymmetric distributions in order to discuss the significance of this value.

Concluding remarks

The study of isothermal crystallization process of itPS by SAXS has revealed that the corrections for the foreign particle component as well as the density fluctuation component are necessary to obtain the quantitative intensity due to the lamellar structure. The interface distribution function provides useful information in choosing an appropriate structure model, though it was difficult to directly determine the values of structure parameters by itself. In the present study, the experimental SAXS intensity has been satisfactorily reproduced by the Gaussian correlation model.

The refinement of a structure model involves the effects of the asymmetry of distance distributions and the improvement of the linear model. The asymmetry of distance distributions may become important depending on the crystallization conditions and on the kinds of substances. In this case, the first minimum in an interface distribution function will give the peak value of distribution of the smaller of crystal thickness and amorphous one, rather than the average value. Electron microscopy shows, in the melt crystallization, that lamellae usually well develop in a parallel direction to the boundary surfaces and a large number of lamellae stack each other, but at the same time, that they are always curved and often branch to be nonparallel in a large scale. The effects of deviations from the linear model is important at large distances in interface distribution functions and correlation functions [10, 17], and hence at smaller scattering angles. The concept of the "locally oriented correlation function" introduced by Vonk [18] will be a useful tool in theoretical treatments and experimental studies at smaller scattering angles and on oriented samples will be necessary in investigating the effects of deviations from the linear model.

Additional parameters must be introduced in order to improve a structure model, but the assessment of the values of parameters obtained becomes more difficult as the number of parameters increases. An accurate interface distribution function could indicate the important factors to be taken into account, such as the correlations between distributions, the shapes of distributions, the finite size of lamellar stacks, and hence the number of structure parameters should be minimized. Only an approximate interface distribution function is obtained in this study because of the limited range of s-values available for a Fourier transformation. An alternative method such as the maximum entropy method is desired to obtain better values for interface distribution functions.

Acknowledgement The authors wish to thank the committee of HIX-LAB of Kyoto University for the use of the SAXS system.

References

1. Tanzawa Y, Miyaji H, Miyamoto Y, Kiho H (1988) Polymer 29:904
2. Tanzawa Y (1992) Polymer 33:2659
3. Miyamoto Y, Tanzawa Y, Miyaji H, Kiho H (1992) Polymer 33:2496
4. Izumi K, Gan Ping, Toda A, Miyaji H, Miyamoto Y (1992) Jpn J Appl Phys 31:L626
5. Vonk CG (1973) J Appl Cryst 6:81
6. Ruland W (1977) Colloid Polym Sci 255:417
7. Wendorff JH, Fischer EW (1973) Kolloid Z Z Polym 251:884
8. Hosemann R, Bagchi SN (1962) Direct Analyses of Diffraction by Matter, North-Holland pp 410
9. Vonk CG, Kortleve G (1962) Kolloid Z Z Polym 220:19
10. Strobl GR, Schneider M (1980) J Polym Sci Polym Phys Ed 18:1343
11. Balta-Calleja FJ, Vonk CG (1989) X-ray Scattering of Synthetic Polymers Elsevier Chapter 7
12. Fiedel HW, Wenig W (1989) Colloid Polym Sci 267:389
13. Stribeck N (1993) Colloid Polym Sci 271:1007

14. Hayashi H, Hamada F, Suehiro S, Masaki N, Ogawa T, Miyaji H (1988) J Appl Cryst 21:330
15. Rathje J, Ruland W (1976) Colloid Polym Sci 254:358
16. Ruland W (1977) Pure Appl Chem 49:905
17. Stribeck N, Ruland W (1978) J Appl Cryst 11:535
18. Vonk CG (1978) J Appl Cryst 11:541
19. Warner FP, MacKnight WJ, Stein RS (1977) J Polym Sci Polym Phys Ed 15:2113
20. Bassett DC, Vaughan AS (1985) Polymer 26:717
21. Vaughan AS, Bassett DC (1988) Polymer 29:1397
22. Blundell DJ (1978) Polymer 19:1258
23. Fukao K, Miyamoto Y (1993) Polymer 34:238